Strojnícky časopis – *Journal of* MECHANICAL ENGINEERING,
VOL 73 (2023), NO 1, 137 - 146

EFFECT OF MISALIGNMENT OF AXES IN DOUBLE-SIDED WELD ON STRESSES DISTRIBUTION IN BUTT WELDED JOINTS

MOLTASOV Andrii[1], TKACH Pavlo[1], USTYNENKO Oleksandr[2], PROTASOV Roman[3]

[1] E.O. Paton Electric Welding Institute of the National Academy of Sciences of Ukraine, Department of Strength of Welded Structures, Kazymyra Malevycha str. 11, 03150 Kyiv, Ukraine
[2] National Technical University "Kharkiv Polytechnic Institute", Institute of Education and Science in Mechanical Engineering and Transport, Department of Theory and Computer-Aided Design of Mechanisms and Machines, Kyrpychova str. 2, 61002 Kharkiv, Ukraine33
[3] Slovak University of Technology in Bratislava, Faculty of Mechanical Engineering, Institute of Transport Technology and Engineering Design, Nám. Slobody 17, 812 31 Bratislava, Slovakia

Abstract: An analytical method for calculation of local stresses in double-sided butt welded joints at misalignment of welds' axes is developed. The method is applicable for welded thin-gauge plates with different geometry of welds on the face and root sides under tensile load. In the given calculation example, it was shown that the stresses reach their maximum value in the zone of transition from the root weld to the base metal which is farther from the axis of the face weld. The results of analytical calculations are in good agreement with the results obtained using the finite element method.

KEYWORDS: butt welded joint, asymmetrical reinforcement, stress condition, stress distribution, root weld reinforcement, misalignment of welds' axes, nonplanar section hypothesis.

1 Introduction

The main reason of MIG butt welded joints' fatigue life limitation is a high level of stresses, caused by weld geometry [1]. Moreover, it is known from [2] that plasticity characteristics are significantly decreasing when the stress concentration level is increasing. As a result, the failure in stress concentration zones occurs at static load as well. The results of tensile tests of butt welded specimens made of high strength aluminium alloys 1460T1 [3] and 2219T8 [4] show that failure occurs in fusion zone (FZ), where the level of stress concentration is the highest. Other research [5, 6] also showed that geometrical characteristics of the weld define the distribution of local stresses and therefore significantly effect on mechanical properties of butt joints produced by fusion welding. The highest value of local stress acting in FZ is the main characteristic that effects on fatigue life of welded joint. This is why stresses concentration and their distribution in the weakest sections are to be defined for fatigue analysis [7].

If the geometric parameters of butt joint allow it to be approximated by finite-element mesh, the value of local stresses can be calculated using the finite element method (FEM). But in the case of sharp notch the stress gradient is high and the stresses values calculated using FEM are sensitive to mesh size. This is why the high value of calculation error is possible [8]. Due to the difficulties in definition of singularity in the zone of transition from the weld to the base metal, in some cases FEM is not applicable for correct calculation of maximal local stresses [9, 10, 11]. This is why authors of [12] proposed the modern two-stage method for calculation of local stresses in butt welded joints. The first stage involves definition of nominal stresses near the weld using FEM. On the second stage the nominal value of stress is to be multiplied by stress

DOI: 10.2478/scjme-2023-0011, Print ISSN 0039-2472, On-line ISSN 2450-5471

concentration factor (SCF) which can be calculated by an appropriate analytical method. For thin-gauge butt welded joints the values of reinforcement height and plate thickness are comparable [13]. This geometrical feature leads to the eccentricity of axial load and, consequently, to emergence of bending stresses which are put together with tensile ones on the root side [14]. Thus the maximal value of local stresses is in FZ of root-side weld. This is confirmed by the results of fatigue tests carried out on MIG-welded butt joints of aluminium alloys 1420 (δ=1.8 mm) and 1460 (δ=2.0 mm) where fatigue crack initiated in the root-side FZ under axial load [15]. The proposed methods for optimizing a welded joint in order to reduce the negative effect of residual stresses suggest a too general approach without taking into account the geometry of the welded joint [16].

An analytical method for SCF calculation [17] was developed based on the assumption that the axis of the root weld coincides with the axis of the face weld. But for real joints this is not always the case, and the axis of the root weld is offset by some eccentricity distance from the axis of the face weld (Fig. 1) [18].

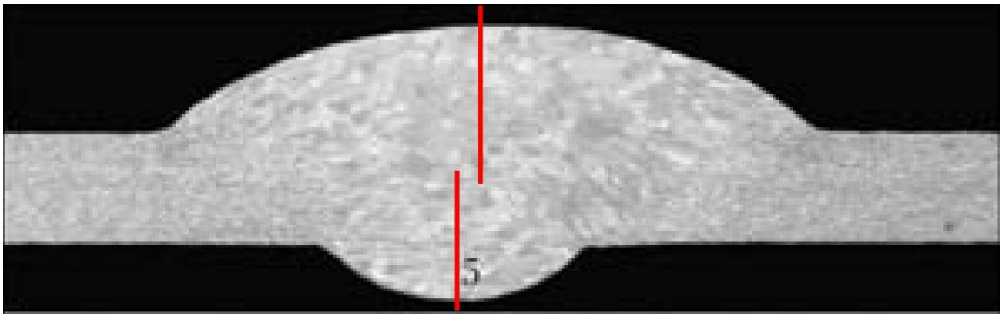


Fig. 1 Macrosection of butt-welded joint produced using MIG Pulse process [16]

Obviously, stress conditions of transition zones from the root weld to the base metal on the left and right sides are different. This is why the method for stress calculation, taking into account the distance between axes of symmetry (distance between red lines on Fig. 1), is needed.

2 Model description

The ideal geometrical model of welds and transition zones, where they are approximated by the arc of circles, will be used (Fig. 2). This approximation model provides good agreement with the real shape of butt welded joint [19].

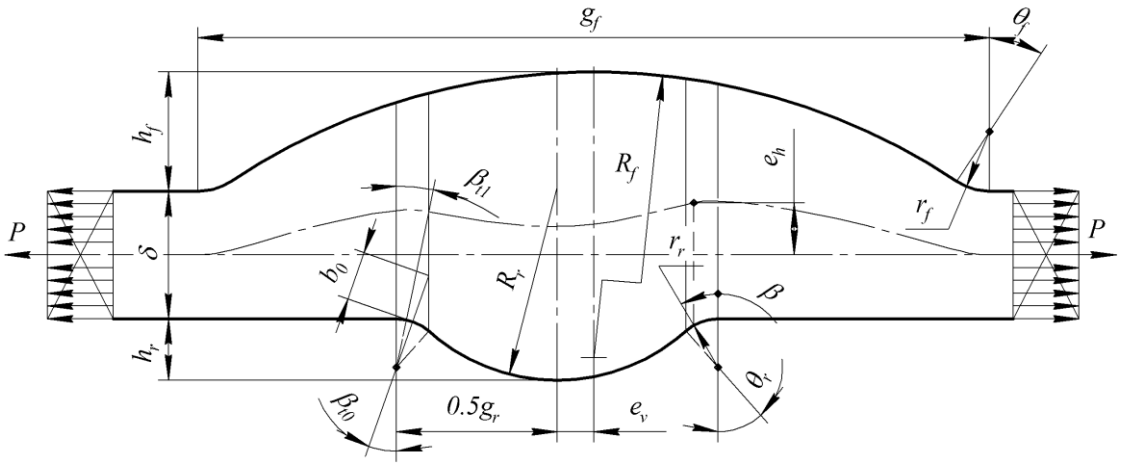


Fig. 2 Geometrical parameters of the ideal model of butt welded joint with shifted face and root welds

Let us draw a nonplanar section *ABC* through point *A* (Fig. 3) in such a way that the segment *AB* of the section is perpendicular to the contour, while the segment *BC* is perpendicular to the line of the load action.

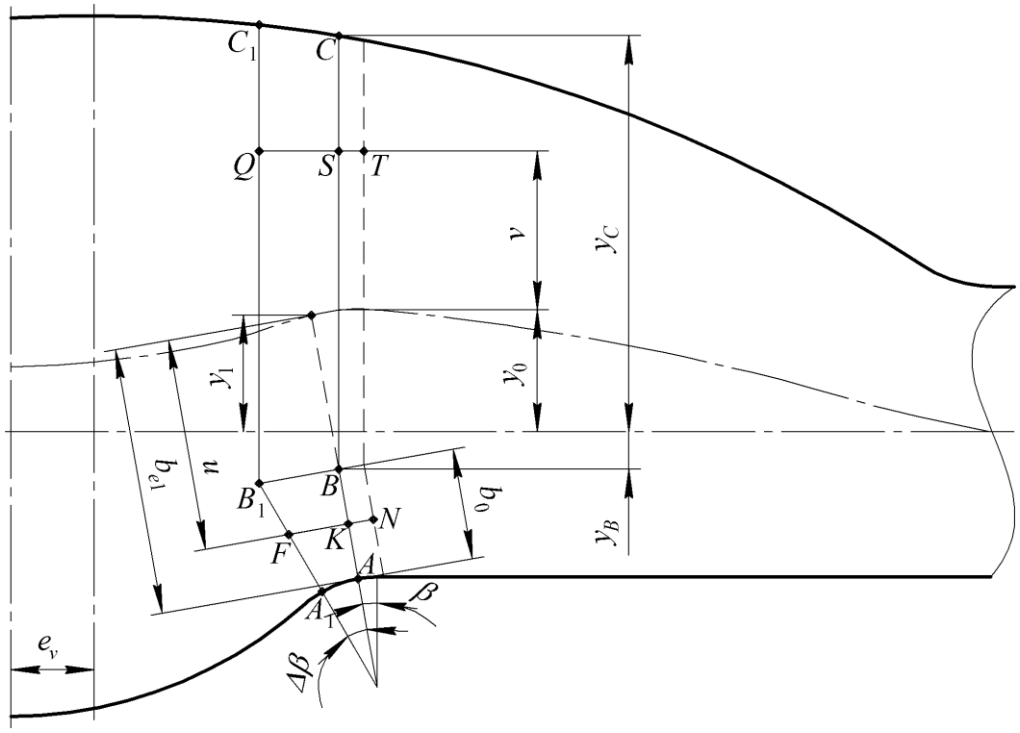


Fig. 3 Creation of nonplanar section closer to the axis of symmetry of the face-side weld

The length of *AB* is equal to depth b_0 of the stress concentration action. It should be noted that the point *A* is located on the contour's side which is closer to the axis of symmetry of the face-side weld. Depth b_0 for ideal model (Fig. 2) can be defined using the results of work [16]:

$$b_0 = 4r_r h_r \sqrt{\frac{2}{g_r^2+4h_r^2}},$$

where r_r is the radius of transition from the weld root reinforcement to the base metal; g_r and h_r are the width and height of the root reinforcement respectively.

Let us draw a nonplanar section $A_1B_1C_1$ following the same rule through the point A_1 in a way that the continuations of the segments *AB* and A_1B_1 form an infinitely small angle $\Delta\beta$ (Fig. 3).

The similar construction of the sections *ABC* and $A_1B_1C_1$ can be made on the contour's side which is farther from the axis of symmetry of the face-side weld.

3 Tensile stresses

According to the results of [16], the displacement of the section *ABC* to the position indicated in Fig. 1 by the dotted line, causes normal tensile stresses in *KF* and *QS* fibers which can be obtained as follows:

$$\sigma_u^T = \frac{KN \cdot E}{(r_r+b_{e1}-u)\cdot\Delta\beta};\ \sigma_v^T = \frac{KN \cdot E}{(r_r+b_0)\cdot\Delta\beta}, \quad (1)$$

where $b_{e1} = \frac{\delta+2y_1+2r_r\cdot(1-\cos\beta)}{2\cos\beta}$.

If the continuation of the segment *AB* intersects the centers-of-inertia line in the root reinforcement transition zone, the following condition is fulfilled:

$$\beta \le \beta_{t1} = arctan \frac{2r_r \cdot sin\theta_r}{\delta + h_f - R_f + r_r(1+cos\theta_r) + \sqrt{R_f^2 - \left(r_r \cdot sin\theta_r - \frac{g_r}{2} \pm e_v\right)^2}}, \quad (2)$$

where δ is the thickness of the base metal; R_f and h_f are the radius of the convex part of the face reinforcement and its height respectively; θ_r is the flank angle on the root side of the weld; and e_v is the distance from the root weld's axis of symmetry to the face weld's axis of symmetry (Fig. 2).

In Eq. (2) and the following formulas, the upper sign before the eccentricity e_v corresponds to the transition zone which is closer to the axis of symmetry of the face-side weld, while the lower sign corresponds to the zone which is farther from the symmetry axis of the face-side weld.

In this case, the parameter y_1 (Fig. 2) can be calculated by the formula [16], taking into account the parameter e_v, as follows:

$$y_1 = \frac{1}{2}\left(\sqrt{\frac{C_{t3}^2}{4} - C_{t2} + \Psi_t} - \frac{C_{t3}}{2} + \sqrt{\left(\frac{C_{t3}}{2} - \sqrt{\frac{C_{t3}^2}{4} - C_{t2} + \Psi_t}\right)^2 + 4\sqrt{\frac{\Psi_t^2}{4} - C_{t0}} - 2\Psi_t}\right)$$

where $\Psi_t = \frac{C_{t2}}{3} + \sqrt[3]{-\frac{C_{tq}}{2} + \sqrt{\frac{C_{tq}^2}{4} + \frac{C_{tp}^3}{27}}} + \sqrt[3]{-\frac{C_{tq}}{2} - \sqrt{\frac{C_{tq}^2}{4} + \frac{C_{tp}^3}{27}}}$; (3)

$$C_{tp} = -\frac{C_{t2}^2}{3} + C_{t1}C_{t3} - 4C_{t0};\ C_{tq} = -\frac{2C_{t2}^3}{27} + \frac{C_{t1}C_{t2}C_{t3}}{3} + \frac{8C_{t0}C_{t2}}{3} - C_{t0}C_{t3}^2 - C_{t1}^2;$$

$$C_{t0} = \frac{\left[4H_t^2 + (g_r \mp 2e_v)^2\right]\left(r_r + \frac{\delta}{2}\right)^2 tan^2\,\beta + 2(g_r \mp 2e_v)(K_t - H_t^2)\left(r_r + \frac{\delta}{2}\right) tan\,\beta - 2(2r_r^2 + K_t)H_t^2 - K_t^2 - H_t^4}{16(1+tan^2\,\beta)};$$

$$C_{t1} = \frac{2\left[4H_t^2 - 8H_t\left(r_r + \frac{\delta}{2}\right) + (g_r \mp 2e_v)^2\right]\left(r_r + \frac{\delta}{2}\right) tan^2\,\beta + 2(g_r \mp 2e_v)\left[4H_t\left(r_r + \frac{\delta}{2}\right) - H_t^2 + K_t\right] tan\,\beta + 8H_t(2r_r^2 + K_t - H_t^2)}{16(1+tan^2\,\beta)};$$

$$C_{t2} = \frac{\left(4\left[(H_t - 2r_r - \delta)^2 - 2H_t(2r_r + \delta)\right] + (g_r \mp 2e_v)^2\right) tan^2\,\beta + 8(g_r \mp 2e_v)\left(H_t - r_r - \frac{\delta}{2}\right) tan\,\beta - 8(2r_r^2 + K_t - 3H_t^2)}{16(1+tan^2\,\beta)};$$

$$C_{t3} = \frac{2(2r_r + \delta - H_t)\,tan^2\,\beta - (g_r \mp 2e_v)\,tan\,\beta - 4H_t}{2(1+tan^2\,\beta)};\ H_t = h_f - R_f - r_r;\ \ K_t = R_f^2 - r_r^2 - \frac{(g_r \mp 2e_v)^2}{4}.$$

If the continuation of the segment *AB* intersects the centers-of-inertia line on the convex part of the root reinforcement, i.e. condition of Eq. (2) is not fulfilled, the parameter y_1 can be defined taking into account the results of [16] as follows:

$$y_1 = \frac{1}{2}\left(\sqrt{\frac{C_{c3}^2}{4} - C_{c2} + \Psi_c} - \frac{C_{c3}}{2} - \sqrt{\left(\frac{C_{c3}}{2} - \sqrt{\frac{C_{c3}^2}{4} - C_{c2} + \Psi_c}\right)^2 + 4\sqrt{\frac{\Psi_c^2}{4} - C_{c0}} - 2\Psi_c}\right).$$

The parameter Ψ_c is defined similarly to Ψ_t with appropriate replacement of C_{tq}, C_{tp}, C_{t0}, …, C_{t3} in Eq. (3) by C_{cq}, C_{cp}, C_{c0}, …, C_{c3}. The parameters C_{c0}, …, C_{c3} which depend on eccentricity e_v can be calculated as follows:

$$C_{c0} = \frac{4\left(H_c^2 + e_v^2\right)\left(r_r + \frac{\delta}{2}\right)^2 tan^2\,\beta - 4\left[(g_r \mp e_v)H_c^2 \pm e_v K_c\right]\left(r_r + \frac{\delta}{2}\right) tan\,\beta + \left[2K_c + H_c^2 - 4R_f^2 + (g_r \mp e_v)^2\right] \cdot H_c^2 + K_c^2}{16(1+tan^2\,\beta)};$$

$$C_{c1} = \frac{2\left[H_c^2+H_c(2r_r+\delta)+e_v^2\right]\left(r_r+\frac{\delta}{2}\right)tan^2\,\beta-\left[H_c^2(g_r\mp e_v)+4H_c\left(r_r+\frac{\delta}{2}\right)(g_r\mp e_v)\pm e_vK_c\right]tan\,\beta-H_c\left[2K_c+2H_c^2-4R_f^2+(g_r\mp 2e_v)\right]}{4(1+tan^2\,\beta)};$$

$$C_{c2} = \frac{\left[(H_c+2r_r+\delta)^2+2H_c(2r_r+\delta)+e_v^2\right]tan^2\,\beta-4(g_r\mp e_v)\left(H_c+r_r+\frac{\delta}{2}\right)tan\,\beta+2K_c+6H_c^2-4R_f^2+(g_r\mp 2e_v)^2}{4(1+tan^2\,\beta)};$$

$$C_{c3} = \frac{(2r_r+\delta+H_c)\cdot tan^2\,\beta-(g_r\mp e_v)\cdot tan\,\beta+2H_c}{1+tan^2\,\beta};\; H_c = R_f - h_f - R_r + h_r;\; K_c = R_f^2 - R_r^2 \pm e_v(g_r \mp e_v),$$

where R_r is the radius of the face weld.

The condition of equilibrium of unit-thickness joint has the form [16]:

$$P = \int_{b_{e1}-b_0}^{b_{e1}} \sigma_u^T\, cos\,\beta\, du + \int_{-y_B-y_0}^{y_C-y_0} \sigma_v^T\, dv, \tag{4}$$

where y_B is defined in [16], while y_C can be calculated, taking into account the eccentricity e_v, as follows:

$$y_C = \frac{\delta}{2} + h_f - R_f + \sqrt{R_f^2 - \left[(r_r + b_0)\,sin\,\beta - \frac{g_r}{2} \pm e_v\right]^2}\,.$$

If the segment *BC* intersects the centers-of-inertia line in the concave part of the root reinforcement, i.e. in the transition zone, the followed condition is fulfilled:

$$\beta \le \beta_{t0} = arcsin\frac{r_r sin\theta_r}{r_r+b_0} \tag{5}$$

and the parameter y_0 can be calculated by the followed formula:

$$y_0 = \frac{1}{2}\left(h_f - R_f - r_r + \sqrt{R_f^2 - \left[(r_r + b_0)\,sin\,\beta - \frac{g_r}{2} \pm e_v\right]^2} + \sqrt{r_r^2 - (r_r + b_0)^2\,sin^2\,\beta}\right).$$

If the segment *BC* intersects the centers-of-inertia line in the convex part of the root reinforcement, i.e. in the root weld zone, the condition of Eq. (5) is not fulfilled, and the parameter y_0 can be calculated as follows:

$$y_0 = \frac{1}{2}\left(h_f - R_f - h_r + R_r + \sqrt{R_f^2 - \left[(r_r + b_0)\,sin\,\beta - \frac{g_r}{2} \pm e_v\right]^2} - \sqrt{R_r^2 - \left[(r_r + b_0)\,sin\,\beta - \frac{g_r}{2}\right]^2}\right).$$

After appropriate substitution of the stresses from Eq. (1) into equilibrium condition (4) and further integration, the calculation formulas for tensile stresses, acting on the transition zones surfaces, can be obtained as follows:

$$\sigma_r^T = \frac{P}{r_r\cdot\left(cos\,\beta\cdot ln\frac{r_r+b_0}{r_r}+\frac{y_C+y_B}{r_r+b_0}\right)} \text{ at } b_0 \le b_{e1};$$

$$\sigma_r^T = \frac{P}{r_r\cdot\left(cos\,\beta\cdot ln\frac{r_r+b_{e1}}{r_r}+\frac{y_C-y_1}{r_r+b_{e1}}\right)} \text{ at } b_0 > b_{e1}.$$

4 Bending stresses

The bending moment M acting in the transition zone from the root weld to the base metal can be defined as follows:

$$M = P \cdot e_h,$$

where e_h is the eccentricity of the tensile load P in the mentioned zone. According to the geometrical model (Fig. 2) the eccentricity can be defined as follows:

$$e_h = \frac{1}{2}\left[h_f - R_f + \sqrt{R_f^2 - \left(r_r \cdot \sin\beta - \frac{g_r}{2} \pm e_v\right)^2} - r_r \cdot (1 - \cos\beta)\right].$$

Let us assume that the section $A_1B_1C_1$ remains stationary under the bending loading, while the section ABC rotates by the small angle $\Delta\gamma$ and occupy a new position which is indicated in Fig. 4 by the dotted line.

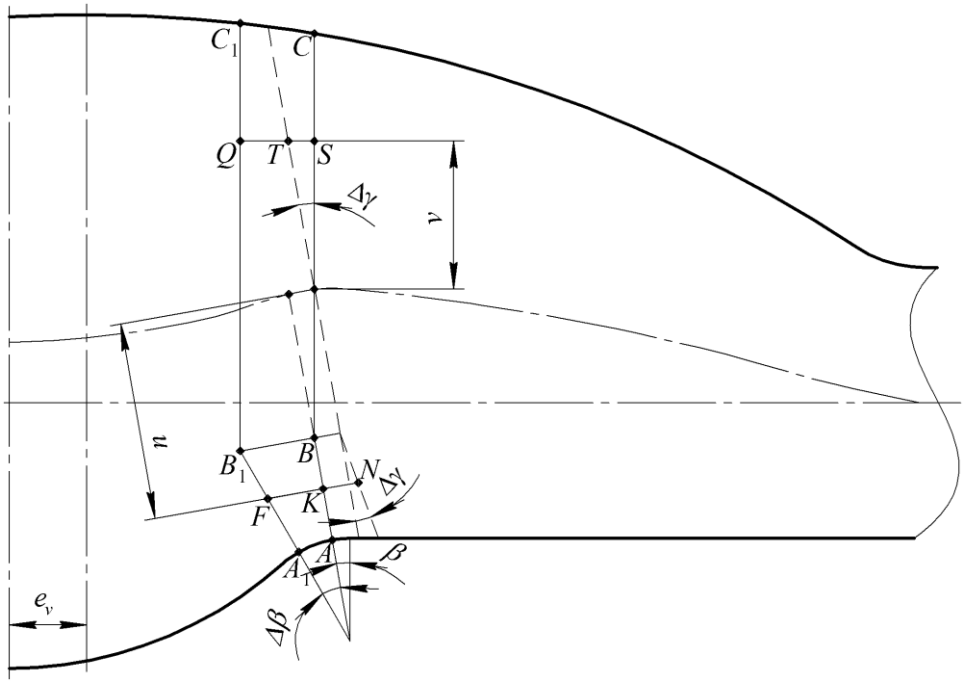


Fig. 4 Rotation of the nonplanar section *ABC* at bending of the butt welded joint

In this case, the fiber KF, which is located at distance u from the center-of-inertia line, will be elongated by the length of the segment KN. As a result, the normal tensile stress will appear in it [16]:

$$\sigma_u^B = \frac{\left(\frac{y_B + y_0}{\cos\beta} + u - b_{e1} + b_0\right) \cdot \Delta\gamma \cdot E}{(r_r + b_{e1} - u) \cdot \Delta\beta}, \tag{6}$$

The length of the segment KN can be defined according to the constructions on Fig. 3 and Fig. 4 as it obtained in [16].

The fiber *QS* located at the distance v from the center-of-inertia line will be shortened by the length of the segment *ST*. The normal compressive stress will appear in it [16]:

$$\sigma_v^B = \frac{v \cdot \Delta\gamma \cdot E}{(r_r + b_0) \cdot \Delta\beta \cdot \cos\beta}. \tag{7}$$

The condition of equilibrium of unit-thickness joint under bending loading has the form which was obtained in [16]:

$$M = \int_{b_{e1} - b_0}^{b_{e1}} \sigma_u^B \cdot \left(\frac{y_B + y_0}{\cos\beta} + u - b_{e1} + b_0\right) du + \int_{-y_B - y_0}^{y_C - y_0} \sigma_v^B \cdot v dv. \tag{8}$$

Let us substitute Eqs. (6) and (7) into equilibrium condition (8) and in a similar manner to [16], after integration formulas for bending stresses acting on the transition zones surfaces can be obtained as follows:

$$\sigma_r^B = \frac{M\cdot(y_B+y_0+b_0\cdot cos\,\beta)}{r_r\cdot B_0\cdot cos\,\beta} \text{ at } b_0 \le b_{e1};$$

$$\sigma_r^B = \frac{M\cdot b_{e1}}{r_r\cdot B_1} \text{ at } b_0 > b_{e1},$$

where parameters B_0 and B_1 can be defined by formulas of [16].

The sum of stresses acting on the transition zones surfaces can be define as follows

$$\sigma_r^\Sigma = \frac{P}{r_r}\left(\frac{1}{T_0} + \frac{e_h\cdot(y_B+y_0+b_0\cdot cos\,\beta)}{B_0\cdot cos\,\beta}\right) \text{ at } b_0 \le b_{e1}; \quad (9)$$

$$\sigma_r^\Sigma = \frac{P}{r_r}\left(\frac{1}{T_1} + \frac{e_h\cdot b_{e1}}{B_1}\right) \text{ at } b_0 > b_{e1}. \quad (10)$$

5 Calculation example

Let us calculate the total stresses for AMg6 aluminium alloy thin plates which were welded by MIG Pulse welding using SvAMg6 wire with the diameter of 1.2 mm. The thickness of welded plates is 1.5 mm and the geometrical shape of the joint is presented on Fig. 1. The geometric parameters of the joint calculated using the ideal model (Fig. 2) are listed below.

Side	Height *h*, mm	Width *g*, mm	Angle θ, °	Radius *r*, mm	Radius *R*, mm
Face (f)	1.400	9.300	33.511	0.700	7.722
Root (r)	0.720	3.780	41.710	0.570	2.271

Based on the measurement of the macrosection of butt-welded joint presented on Fig. 1 the value of eccentricity of $e_v = 0.430$ mm was obtained.

The value of depth of the stress concentration action in transition zone from the root weld to the base metal is $b_0 = 0.574$ mm. Since in the border point of the zone, i.e. at $\beta = 0°$, condition $b_0 \le \delta/2$ is fulfilled, obviously, the condition is also fulfilled at $0° \le \beta \le \theta_r$. This is why Eq. (9) was used for stresses calculation.

6 Results analysis

Let us draw the stress diagrams by values calculated using Eq. (9) for the root side of the joint (Fig. 5).

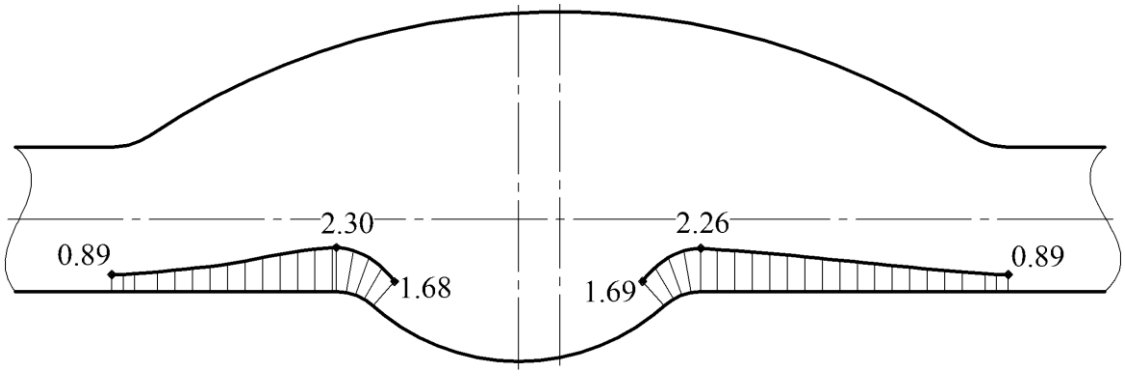


Fig. 5 Stress diagrams on the root side of the joint with shifted axes of symmetry of welds

It was considered in local stress calculation that the joint in Fig. 5 is loaded in such a way that the value of nominal stress in the plate, i.e. far from the weld, is $\sigma_{nom} = 1$Pa.

The value of eccentricity e_h in the border point of the transition zone which is farther from the axis of symmetry of the face weld (left border point) is $e_{hl} = 0.52$ mm. This value is less than in the border point of the transition zone which is closer to the axis of symmetry of the face weld (right border point) $e_{hr} = 0.63$ mm. This is why the highest value is expected to be on the right side.

But the analysis of diagrams in Fig. 5 shows that the highest stress value is in the left border point. This is due to the fact that the eccentricity e_h is increased when increasing the face-side reinforcement height, but, at the same time, the cross-sectional area increases as well. The results of research [20] show that enlargement of the cross section due to the face-side reinforcement height increasing leads to declination of stress value in the root-side transition zone.

Computer simulation of stress condition using the finite element method (FEM) was carried out (Fig. 6) for calculation results (Fig. 5) verification.

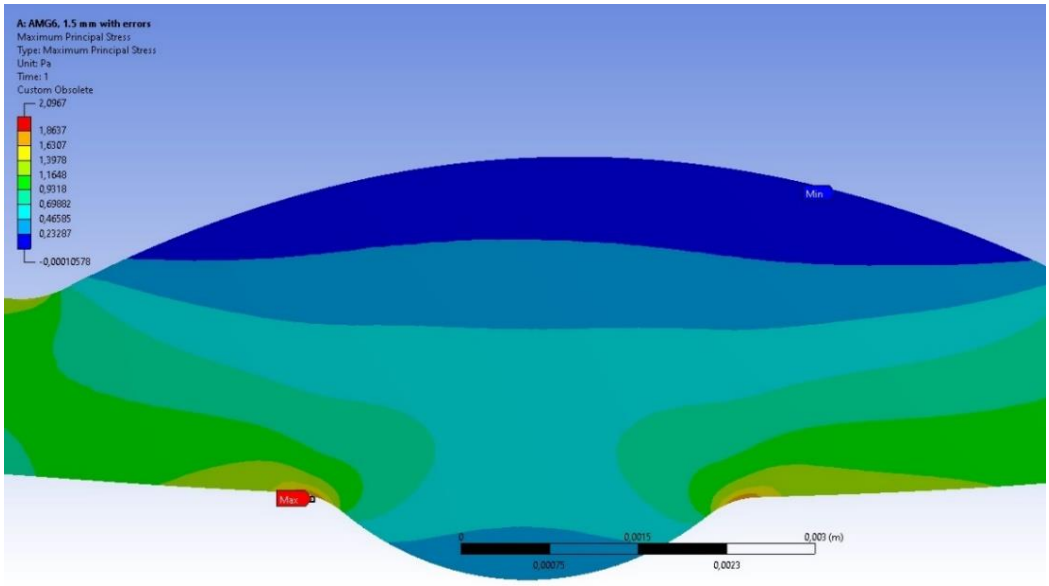


Fig. 6 Results of stress fields numerical simulation in AMg6 alloy butt welded joint

The finite element model of the test specimen was obtained based on dimensions shown in the table. In order to exclude influence of the mesh size on the values of local stresses, the mesh was refined until the difference between the stress values in the final and previous model was obtained, not exceeding 5%. The final model included 67,726 elements with 262,039 nodes. The element size in the transition zones was chosen less than 0.1 of the transition radius r_r, i.e. 0.05 mm.

The maximum value of the principal stress according to the analytical calculation is obtained in the transition zone which is farther from the axis of the face weld (Fig. 5), at $\beta = 0$. This is confirmed by the results of computer simulation of stress fields which is shown in Fig. 6. The stresses distribution along the contour of the joint is the same. The deviations of the maximum stress values, obtained by the analytical and numerical calculations, are less than 10%.

The value of SCF is defined as the ratio of the stress determined by Eq. (9) at $\beta = 0$ to the nominal stress $\sigma_{nom} = P/\delta$ (for the weld of unit length) which acts far from the weld. Taking into account that $y_1 = y_0$ and $b_{e1} = \delta/2 + y_0$ at $\beta = 0$ for the case of $b_0 \le b_{e1}$ we obtain:

$$\alpha_\sigma^r = \frac{\delta}{r_r}\left(\frac{1}{ln\frac{r_r+b_0}{r_r}+\frac{m-b_0}{r_r+b_0}} + \frac{m\cdot(m-\delta)}{4\left[\left(r_r+\frac{m}{2}\right)^2 ln\frac{r_r+b_0}{r_r}-b_0\cdot(r_r+m)+\frac{b_0^2}{2}+\frac{m^3+(m-2b_0)^3}{24(r_r+b_0)}\right]}\right) \quad (11)$$

where $m = \delta + h_f - R_f + \sqrt{R_f^2 - \frac{1}{4}(g_r \mp 2e_v)}$.

If the condition $b_0 > b_{e1}$ is fulfilled, the value of SCF can be defined as the ratio of the stress determined by Eq. (10) at $\beta = 0$ to the nominal stress:

$$\alpha_\sigma^r = \frac{\delta}{r_r}\left(\frac{1}{ln\frac{2r_r+m}{2r_r}+\frac{m}{2r_r+m}} + \frac{m\cdot(m-\delta)}{4\left[\left(r_r+\frac{m}{2}\right)^2 ln\frac{2r_r+m}{2r_r}-\frac{m}{2}\cdot(r_r+m)+\frac{m^2}{8}+\frac{m^3}{12(2r_r+m)}\right]}\right) \quad (12)$$

It should be noted that when there is no eccentricity, i.e. at $e_v = 0$, Eqs. (11) and (12) are identical to appropriate formulas from [15].

CONCLUSION

The analytical method for assessment of the stress condition and SCF calculation under the tensile load in the stress concentration zones is developed and verified. The method is applicable for the butt welded joint with shifted face and root welds, i.e. with eccentricity of welds. The following conclusions can be drawn:

1. The results of calculation by the method show that the maximum transition zone stress acts in the side which is farther from the axis of the face weld. This fact can be explained by the dimension of the cross-section on this side which is less than on the opposite side.
2. The obtained results were confirmed by the results of the stress numerical analysis: the stresses distributions along the contour of the joint obtained analytically and using FEM are the same. The maximum stress value obtained using FEM differ from calculated one is less than 10%.
3. Due to the ability of the obtained formulas to consider the value of eccentricity of the face and root welds, the developed method allows to obtain more accurate values of local stresses in stress concentration zone of butt welded joints.

REFERENCES

[1] Motrunich, S., Poklatsky, A., Klochkov, I., Rogante, M., Zavdoveev, A. "Basic advantages of thin-sheet AA5056 alloy joints produced by friction stir welding", Proc. of the 10th International Conference on Mechanical Technologies and Structural Materials, MTSM 2021, Split, Croatia, 2021 (70), pp. 119 – 124, **2021**. ISSN 18477917

[2] Vorob'ev, E. V., Strizhalo, V. A., Anpilogova, T. V. "Strain-hardening of notched steel specimens during their deep cooling down to 4.2 K", Strength of Materials 49 (5), pp. 613 – 617, **2017**. DOI: 10.1007/s11223-017-9906-0

[3] Lukinenko, A. O., Motrunich, S. I., Bajic, D., Kuleshov, V. A., Pokliatskyi, A. G., Labur, T. M. "Noise level assessment and mechanical properties of welded joints of aluminium alloys of the Al-Cu-Li system in FSW and TIG welding", FME Transactions 49 (1), pp. 220 – 224, **2020**. DOI: 10.5937/FME2101220L

[4] Wan, Z., Meng, D., Zhao, Y., Zhang, D., Wang, Q., Shan, J., Song, J., Wang, G., Wu, A. "Improvement on the tensile properties of 2219-T8 aluminum alloy TIG welding joint with weld geometry optimization", Journal of Manufacturing Processes 67, pp. 275 – 285, **2021**. DOI: 10.1016/j.jmapro.2021.04.062

[5] Wang, G., Li, Q., Li, J., Wu, A., Ma, N., Yan, D., Wu, H. "Effects of weld reinforcement on tensile behavior and mechanical properties of 2219-T87 aluminum alloy TIG welded joints", Transactions of Nonferrous Metals Society of China 27 (1), pp. 10 – 16, **2017**. DOI: 10.1016/S1003-6326(17)60002-5

[6] Ma, M., Lai, R., Qin, J., Wang, B., Liu, H., Yi, D. "Effect of weld reinforcement on tensile and fatigue properties of 5083 aluminum metal inert gas (MIG) welded joint: Experiments

and numerical simulations", International Journal of Fatigue 144, Article number 106046, **2021**. DOI: 10.1016/j.ijfatigue.2020.106046

[7] Goyal, R., El-Zein, M., Glinka, G. "A robust stress analysis method for fatigue life prediction of welded structures", Welding in the World 60 (2), pp. 299 – 314, **2016**. DOI: 10.1007/s40194-016-0295-y

[8] Lee, J., Seo, J., Kim, M., Shin, S., Han, M., Park, J., Mahendran, M. "Comparison of hot spot stress evaluation methods for welded structures", International Journal of Naval Architecture and Ocean Engineering 2 (4), pp. 200 – 210, **2010**. DOI: 10.3744/JNAOE.2010.2.4.200

[9] Doerk, O., Fricke, W., Weissenborn, C. "Comparison of different calculation methods for structural stresses at welded joints", International Journal of Fatigue 25 (5), pp. 359 – 369, **2003**. DOI: 10.1016/S0142-1123(02)00167-6

[10] Fricke, W., Kahl, A. "Comparison of different structural stress approaches for fatigue assessment of welded ship structures", Marine Structures 18 (7-8), pp. 473 – 488, **2005**. DOI: 10.1016/j.marstruc.2006.02.001

[11] Sejč, P., Világoš, T. "Fem Simulation of Thermal Cycles During Laser Welding of Aluminium" Strojnícky časopis – Journal of Mechanical Engineering 68 (1), pp. 89 – 94, **2018**. DOI: 10.2478/scjme-2018-0009

[12] Goyal, R., El-Zein, M., Glinka, G. "Computational weld analysis and fatigue of welded structures", In: da Silva, L. F. V., El-Zein, M., Martins, P. A. F. (eds) Advanced joining processes. Welding, plastic deformation, and adhesion. Elsevier Inc., Amsterdam, Oxford, Cambridge, First edition, **2021**. DOI: 10.1016/C2019-0-01447-1

[13] Tsumarev, Yu. A. "Effect of off-centre tensile loading on the stress state of butt-welded joints", Welding International 25 (11), pp. 872 – 875, **2011**. DOI: 10.1080/09507116.2011.581426

[14] Moltasov, A. V. "Stressed state of a butt-welded joint with regard for displacements of the centers of inertia", Materials Science 55 (3), pp. 358 – 366, **2019**. DOI: 10.1007/s11003-019-00310-2

[15] Motrunich, S., Klochkov, I., Poklaytsky, A. "High cycle fatigue behaviour of thin sheet joints of aluminium-lithium alloys under constant and variable amplitude loading", Welding in the World 64 (12), pp. 1971 – 1979, **2020**. DOI: 10.1007/s40194-020-00976-2

[16] Élesztős P., Jančo R., Voštiar V. "Optimization of Welding Process using a Genetic Algorithm", Strojnícky časopis – Journal of Mechanical Engineering 68 (2), pp.17 – 24, **2018**. DOI: 10.2478/scjme-2018-0014

[17] Moltasov, A., Tkach, P., Ustynenko, O., Protasov, R. "Effect of load eccentricity on stress condition of butt welded joint with asymmetrical reinforcement", Strojnícky časopis – Journal of Mechanical Engineering 72 (1), pp. 99 – 108, **2022**. DOI: 10.2478/scjme-2022-0010

[18] Mashin, V. S., Pashulya, M. P., Shonin, V. A., Klochkov, I. N. "Consumable electrode pulsed argon-arc welding of sheet aluminium alloys", The Paton Welding Journal, 5, pp. 38 – 41, **2010**. ISSN 0957-798X

[19] Molski, K. L., Tarasiuk, P. "Stress concentration factors for butt-welded plates subjected to tensile, bending and shearing loads", Materials 13 (8), Article number 1798, **2020**. DOI: 10.3390/MA13081798

[20] Moltasov, A. V. "A study of the stress state in stress concentration zones under tension of an asymmetrically reinforced butt-welded joint", Strength of Materials 49(5), pp. 718 – 725, **2017**. DOI: 10.1007/s11223-017-9917-x